



## Mepyramine–JNJ7777120-hybrid compounds show high affinity to hH<sub>1</sub>R, but low affinity to hH<sub>4</sub>R

Eva Wagner<sup>a</sup>, Hans-Joachim Wittmann<sup>b</sup>, Sigurd Elz<sup>a</sup>, Andrea Strasser<sup>c,\*</sup>

<sup>a</sup> Department of Pharmaceutical/Medicinal Chemistry I, Institute of Pharmacy, University of Regensburg, D-93040 Regensburg, Germany

<sup>b</sup> Faculty of Chemistry and Pharmacy, University of Regensburg, D-93040 Regensburg, Germany

<sup>c</sup> Department of Pharmaceutical/Medicinal Chemistry II, Institute of Pharmacy, University of Regensburg, Universitätsstraße 31, D-93040 Regensburg, Germany

### ARTICLE INFO

#### Article history:

Received 15 June 2011

Revised 31 August 2011

Accepted 1 September 2011

Available online 7 September 2011

#### Keywords:

Histamine H<sub>1</sub> receptor

Histamine H<sub>4</sub> receptor

Mepyramine

JNJ7777120

Hybrid compounds

Molecular dynamics

### ABSTRACT

In literature, a synergism between histamine H<sub>1</sub> and H<sub>4</sub> receptor is discussed. Furthermore, it was shown, that the combined application of mepyramine, a H<sub>1</sub> antagonist and JNJ7777120, a H<sub>4</sub> receptor ligand leads to a synergistic effect in the acute murine asthma model. Thus, the aim of this study was to develop new hybrid ligands, containing one H<sub>1</sub> and one H<sub>4</sub> pharmacophor, connected by an appropriate spacer, in order to address both, H<sub>1</sub>R and H<sub>4</sub>R. Within this study, we synthesized nine hybrid compounds, which were pharmacologically characterized at hH<sub>1</sub>R and hH<sub>4</sub>R. The new compounds revealed (high) affinity to hH<sub>1</sub>R, but showed only low affinity to hH<sub>4</sub>R. Additionally, we performed molecular dynamic studies for some selected compounds at hH<sub>1</sub>R, in order to obtain information about the binding mode of these compounds on molecular level.

© 2011 Elsevier Ltd. All rights reserved.

Histamine H<sub>1</sub> receptor antagonists are used in general for the treatment of allergic reactions, whereas the histamine H<sub>4</sub> receptor is suggested to be involved in allergic diseases, like conjunctivitis, rhinitis or bronchial asthma as well as in atopic dermatitis and pruritus.<sup>1–4</sup> Mepyramine **1** (Scheme 1) is a prominent H<sub>1</sub>R antagonist, whereas JNJ7777120 **2** (Scheme 1) shows high affinity to the H<sub>4</sub>R.<sup>4</sup> In 2003 JNJ7777120 **2** was described as a potent and selective H<sub>4</sub> antagonist, which has meanwhile established to a H<sub>4</sub>R standard antagonist.<sup>5</sup> Further studies revealed that JNJ7777120 acts as inverse agonist at hH<sub>4</sub>R but as partial agonist at mH<sub>4</sub>R.<sup>6</sup> Recently, it was shown experimentally, that the combined application of mepyramine **1** and JNJ7777120 **2** in the acute murine asthma model leads to a synergistic effect.<sup>7</sup> Thus, the development of combined H<sub>1</sub>/H<sub>4</sub>-receptor ligands may be a worthwhile goal for treatment of allergic reactions,<sup>1</sup> since differences in bioavailability are expected if two drugs are administered. This is not the case, if H<sub>1</sub>R and H<sub>4</sub>R can be addressed with only one drug. Furthermore, ligands addressing both H<sub>1</sub>R and H<sub>4</sub>R are important pharmacological tools to get deeper insights with regard to ligand binding and selectivity on molecular level. One strategy for development of dual H<sub>1</sub>/H<sub>4</sub>-receptor ligands is the connection of one H<sub>1</sub>- and one H<sub>4</sub>-pharmacophor by a spacer. This concept was already applied by Schunack with regard to H<sub>1</sub>R and H<sub>2</sub>R.<sup>8,9</sup> Since the combined application of mepyramine **1** and JNJ7777120 **2** lead to the synergistic effect in the acute

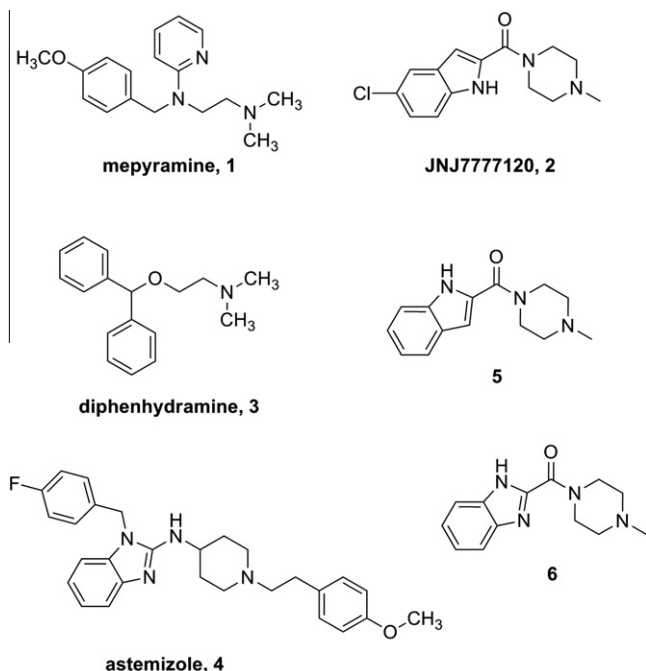
murine asthma model,<sup>7</sup> the aim of this study was to synthesize and pharmacologically characterize a number of compounds, combining mepyramine as H<sub>1</sub>- and JNJ7777120 as H<sub>4</sub>-pharmacophor.

The hybrid ligands **16–21** were obtained as described (Scheme 2). The structures of compounds **26**, **38** and **45** are presented in Scheme 3, whereas the strategy with regard to synthesis can be found in the supplementary material. Further details with regard to synthesis, as well as analytics of all hybrid compounds are given in the supplementary material.

The synthesized compounds were routinely investigated in competition binding assays. In case of hH<sub>1</sub>R, Sf9 cell membranes, coexpressing hH<sub>1</sub>R and RGS4 were used for competition binding assays in presence of 5 nM [<sup>3</sup>H]mepyramine.<sup>10</sup> In case of hH<sub>4</sub>R, Sf9 cell membranes, coexpressing hH<sub>4</sub>R-RGS19, Gα<sub>i2</sub> and Gβ<sub>1</sub>γ<sub>2</sub> were used for competition binding assays in presence of 10 nM [<sup>3</sup>H]histamine.<sup>11</sup> Furthermore, some selected compounds were analyzed at hH<sub>4</sub>R with the GTPγS-assay in order to determine the efficacy.<sup>12</sup> Additionally, most of the new compounds were tested routinely on isolated guinea-pig ileum.<sup>13</sup> Since only H<sub>1</sub>R, but not H<sub>4</sub>R is expressed on ileum, in organ pharmacology, assays at guinea-pig ileum are well established in order to study the affinity and functionality at gpH<sub>1</sub>R. The histamine-induced contraction of the guinea-pig ileum is measured in presence and absence of an antagonist.<sup>13</sup>

Since the new hybrid compounds showed affinity to H<sub>1</sub>R, but did not act as (partial) agonists at H<sub>1</sub>R, a model of hH<sub>1</sub>R in the inactive conformation was generated by homology modelling, based on

\* Corresponding author. Tel.: +49 941 943 4821; fax: +49 941 943 4820.  
E-mail address: [andrea.strasser@chemie.uni-regensburg.de](mailto:andrea.strasser@chemie.uni-regensburg.de) (A. Strasser).



**Scheme 1.** Structures of H<sub>1</sub> (mepyramine, **1**; diphenhydramine, **3**; astemizole, **4**) and H<sub>4</sub> (JNJ777120, **2**; JNJ-derivative, **5**; JNJ-derivative, **6**) receptor ligands.

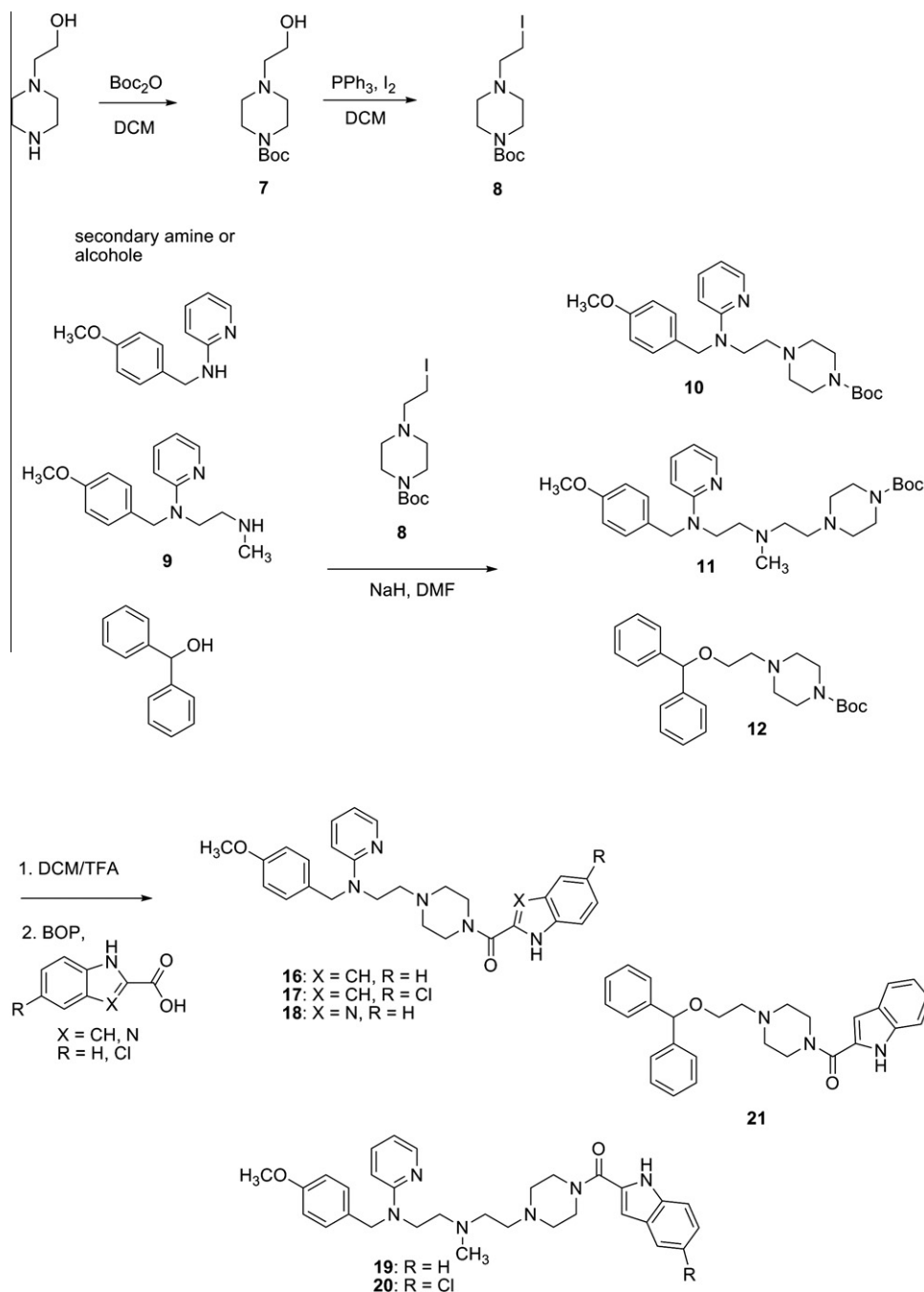
the crystal structure 2RH1,<sup>14</sup> analogue, as already described.<sup>15</sup> A comparison of our H<sub>1</sub>R homology model, refined by molecular dynamic simulations, with the recently published hH<sub>1</sub>R crystal<sup>16</sup> showed no significant differences. The compounds **16**, **19** and **38** were docked manually into the binding pocket of hH<sub>1</sub>R using the software package SYBYL 7.0 (Tripos Inc.). Molecular dynamic simulations, using the software GROMACS 4.0.2 (<http://www.gromacs.org>), were performed, as already described.<sup>10</sup> Ligand parameterization was obtained from the PRODRG server (<http://davapc1.bioch.dundee.ac.uk/prodrg/>). For both compounds a 6 ns productive phase in molecular dynamic simulations was performed subsequent to a 1 ns equilibration phase.

The pharmacological and modeling data of reference compounds and the new hybrid compounds are given in Tables 1–4. For compounds **16** and **19**, the experimental pharmacological data are shown in Figure 1.

Compared to mepyramine, the affinity of compounds **16–18** is significantly reduced of about 1.5–2 log units at hH<sub>1</sub>R. The introduction of one chlorine atom in the indole moiety **17** leads to a slight decrease in affinity to hH<sub>1</sub>R, compared to **16**. The exchange of the indole moiety **16** into a benzimidazole **18** leads to a decrease in affinity at hH<sub>1</sub>R. For compound **19**, an affinity comparable to that of mepyramine **1** at hH<sub>1</sub>R could be observed. The introduction of one chlorine atom on the corresponding position in the JNJ777120 partial structure **20** leads to a significant decrease in affinity at hH<sub>1</sub>R, compared to **19**. In compounds **16–18**, the basic nitrogen atom is embedded in a piperazine moiety, which shows a higher rigidity than an ethylene spacer. This more voluminous piperazine moiety is suggested to disturb the electrostatic interaction between the positively charged amine and Asp<sup>3.32</sup>, leading to a significantly decreased affinity. Based on the molecular dynamic studies, a mean coulomb energy (short range) between **16** and hH<sub>1</sub>R of about  $-157 \pm 1$  kJ/mol was detected (Fig. 2). In contrast, a coulomb energy (short range) of  $-197 \pm 1$  kJ/mol was detected between **19** and hH<sub>1</sub>R (Fig. 2, Table 2). Both interaction energies are, according to a t-test, significant different to each other ( $p < 0.0001$ ). In contrast, there is no significant difference with regard

to the Lennard-Jones energy (short-range) interaction energies between **16** ( $-252 \pm 1$  kJ/mol) or **19** ( $-253 \pm 1$  kJ/mol) and hH<sub>1</sub>R (Table 2). Thus, the dynamic studies support the hypothesis that the piperazine moiety disturbs the electrostatic interaction between **16** and hH<sub>1</sub>R. This difference in the short range coulomb interaction is reflected by the experimentally determined pK<sub>i</sub> values of **16** and **19** at hH<sub>1</sub>R (Fig. 1A). However, during the molecular dynamic simulations, a stable hydrogen bond interaction could be detected between the carbonyl moiety of **16** and Asn<sup>2.61</sup> (Fig. 2). Additionally, an aromatic interaction between the indole moiety of **16** and Tyr<sup>2.64</sup> was observed during the simulation (Fig. 2). In compound **19**, the amino moiety, suggested to interact with Asp<sup>3.32</sup> is flexible, analogous to mepyramine itself and in contrast to compounds **16–18**. Thus, the interaction between the amine moiety and Asp<sup>3.32</sup> can be established well. This is also confirmed by the stronger electrostatic interaction between hH<sub>1</sub>R and **19**, compared to **16** (Fig. 2). However, the elongation of mepyramine by the JNJ777120 partial structure did not lead to an increased affinity at hH<sub>1</sub>R, compared to mepyramine **1**. Since there is a significant difference in affinity of **19** and **20** at hH<sub>1</sub>R, it may be suggested, that the additional JNJ777120 partial structure interacts specifically with the hH<sub>1</sub>R. A stable hydrogen bond was detected during the molecular dynamic simulation between the carbonyl moiety of **19** and Thr182 (E2-loop) (Fig. 2). The exchange of the piperazine moiety by a more flexible aminopyrrolidine moiety **26** leads only to a slight decrease in affinity at hH<sub>1</sub>R, compared to **16**. The diphenhydramine–JNJ-hybrid compound **21**, analogue to the mepyramine–JNJ-hybrid compound **16**, leads to a decrease in affinity of about 1 log unit at hH<sub>1</sub>R, compared to diphenhydramine **3**. For the analogue astemizole–JNJ-hybrid compound **45**, only a slight decrease in affinity was observed at hH<sub>1</sub>R, compared to astemizole **4**. Thus, the introduction of a JNJ partial structure into mepyramine and diphenhydramine leads to a stronger decrease in affinity, compared to the corresponding H<sub>1</sub> antagonists. In contrast, the JNJ–astemizole hybrid shows an affinity in the same range as found for astemizole (Fig. 3). Compound **38** shows a significant decrease in affinity at hH<sub>1</sub>R, compared to **19**. In **38**, the JNJ partial structure is connected to mepyramine via the indole moiety, whereas in **19**, the JNJ partial structure is connected via the piperazine moiety to mepyramine. Thus, this switch is suggested to be responsible for the observed differences in affinity. Compound **38** was obtained experimentally as racemate, but in molecular modelling, both enantiomers were analyzed (Fig. 2). Molecular dynamic simulations revealed a stable binding mode for both enantiomers. The mepyramine partial structure (for both enantiomers) is located in the same part of the binding pocket, as already described for **16** or **19** and the positively charged amino moiety of **38** (both enantiomers) interacts electrostatically with Asp<sup>3.32</sup>. Molecular dynamic simulations revealed a stable hydrogen bond interaction between the carbonyl moiety of **38** (R- and S-configuration) and Trp<sup>7.40</sup>. For **38** (S-configuration), the carbonyl moiety establishes an additional hydrogen bond to Asn<sup>2.61</sup>. Aromatic interactions between the indole moiety of **38** and the receptor were not detected. However, both enantiomers showed slight differences in conformation in its receptor bound state. These differences are reflected in the interaction energy between **38** and hH<sub>1</sub>R. Between the R enantiomer of **38** and hH<sub>1</sub>R, a coulomb energy (short range) of  $-166 \pm 3$  kJ/mol and a Lennard-Jones energy (short range) of  $-285 \pm 2$  kJ/mol was observed. In contrast, between the S enantiomer of **38** and hH<sub>1</sub>R, a coulomb energy (short range) of  $-241 \pm 2$  kJ/mol and a Lennard-Jones (short range) of  $-284 \pm 1$  kJ/mol was observed (Table 2).

As shown in Table 2, a comparison of the calculated ligand-receptor-interaction energies (C+LJ LR, Table 2) does not reflect the observed pK<sub>i</sub> values of **16**, **19** and **38**. However, this observation can be explained: During molecular dynamic simulations, the

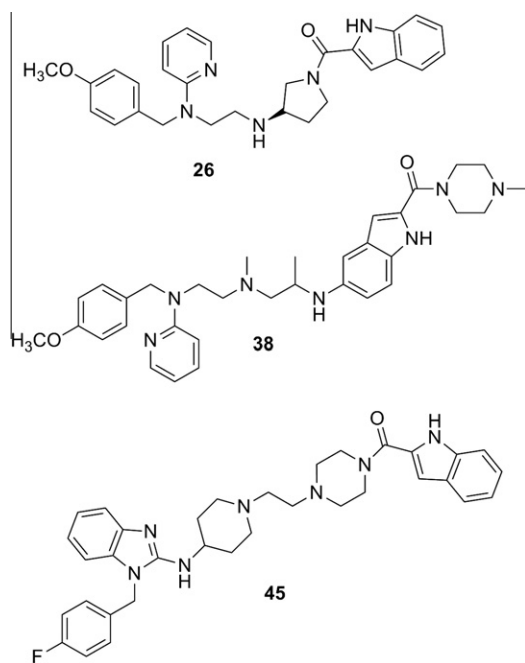


**Scheme 2.** Synthesis of the hybrid compounds **16–21**. A detailed information with regard to synthesis and analytic data is available in the Supplementary data.

penetration of water molecules from the extracellular side into the binding pocket could be observed. These internal water molecules interact with the ligand and with the receptor and mediate ligand–receptor–interactions. Thus, a term, quantifying the interaction between ligand and internal water has to be introduced (Table 2). Taking into account both, interaction of the ligand with the receptor and with the internal water leads to a good correspondence with the experimentally observed  $\text{pK}_i$  values. Additionally, before establishing the ligand–receptor–complex, the ligand is solvated in aqueous solution. Thus, for transfer of the ligand from aqueous solution into the binding pocket of the receptor, changes in solvation energies have to be taken into account. Changes in Gibbs energy of solvation for the ligand can be calculated by molecular dynamic studies.<sup>18</sup>

The predicted changes in Gibbs energy of solvation for the transfer of **16**, **19** and **38** from aqueous phase into binding pocket of  $\text{hH}_1\text{R}$  ( $\Delta G_{\text{sol}}^0$  (water  $\rightarrow$   $\text{hH}_1\text{R}$ )) exhibit a quite well correlation with the experimentally determined  $\text{pK}_i$  values (Table 3). Furthermore, these data reveal also the importance to take into account the Gibbs energy of solvation for the ligand in aqueous solution ( $\Delta G_{\text{sol}}^0$  (L, wat)). Only looking onto  $\Delta G_{\text{sol}}^0$  (L,  $\text{hH}_1\text{R}$ ) would lead to wrong predictions. However, calculations of Gibbs energies of solvation for the transfer of a ligand from aqueous phase into binding pocket of a GPCR are rarely found in literature. Thus, more data have to be obtained in future on different GPCRs in order to judge the predictive quality of such calculations.

None of the hybrid compounds revealed (partial) agonism at  $\text{gpH}_1\text{R}$ . Exemplary for compounds **16** and **19**, the dose-response



**Scheme 3.** Structures of compounds **26**, **38** and **45**. A detailed information with regard to synthesis and analytic data is available in the Supplementary data.

**Table 1**

Binding affinities and functional data of the reference compounds and the hybrid compounds determined in the competition binding assay and on the isolated guinea pig ileum

	$pK_i$ (hH <sub>1</sub> R) (Sf9) <sup>a</sup>	$pK_i$ (hH <sub>4</sub> R) (Sf9) <sup>b</sup>	$pA_2$ (gp-ileum) <sup>c</sup>
Mepyramine, <b>1</b>	$8.35 \pm 0.03^{17}$	$<4^7$	$9.07 \pm 0.03^{13}$
JNJ7777120, <b>2</b>	$4.33 \pm 0.12$	$7.73 \pm 0.04^{11}$	$5.80 \pm 0.13$
Diphenhydramine, <b>3</b>	$7.83 \pm 0.03^{17}$	$4.37 \pm 0.10^7$	$7.93 \pm 0.04^d$
Astemizole, <b>4</b>	$8.68 \pm 0.05$	$5.10 \pm 0.06^7$	$8.42 \pm 0.10$
JNJ derivative, <b>5</b>	n.d.	$6.86 \pm 0.05^{11}$	n.d.
JNJ derivative, <b>6</b>	n.d.	$6.54 \pm 0.04^{11}$	n.d.
<b>16</b>	$6.77 \pm 0.05$	$5.23 \pm 0.09$	$7.97 \pm 0.08$
<b>17</b>	$6.11 \pm 0.08$	$4.80 \pm 0.29$	$7.69 \pm 0.09^d$
<b>18</b>	$6.22 \pm 0.07$	$4.65 \pm 0.04$	$8.14 \pm 0.09$
<b>19</b>	$8.15 \pm 0.10$	$5.05 \pm 0.11$	$8.31 \pm 0.08^d$
<b>20</b>	$7.00 \pm 0.03$	$5.17 \pm 0.09$	$8.12 \pm 0.11^d$
<b>21</b>	$6.65 \pm 0.06$	$4.75 \pm 0.14$	n. d.
<b>26</b>	$6.34 \pm 0.10$	$4.56 \pm 0.09$	$8.07 \pm 0.06$
<b>38</b>	$6.67 \pm 0.09$	$4.85 \pm 0.09$	$7.90 \pm 0.06^d$
<b>45</b>	$8.26 \pm 0.17$	$4.98 \pm 0.04$	$8.42 \pm 0.08^d$

<sup>a</sup> Affinities at hH<sub>1</sub>R, coexpressed with RGS4 in Sf9 cell membranes in the [<sup>3</sup>H]mepyramine competition binding assay.  $K_D$ (mepyramine) at hH<sub>1</sub>R:  $4.49 \pm 0.35$  nM.<sup>10</sup>

<sup>b</sup> Affinities at hH<sub>4</sub>R-RGS19, coexpressed with G $\alpha_{12}$  and G $\beta_{1,2}$  in Sf9 cell membranes in the [<sup>3</sup>H]histamine competition binding assay.  $K_D$ (histamine) at hH<sub>4</sub>R:  $9.8 \pm 0.9$  nM.<sup>6</sup>

<sup>c</sup> Incubation time: 15 min. For most analyzed compounds, a depression in histamine induced contractile effect was observed for higher ligand concentrations. A more detailed description of experimental methods is described by Elz et al.<sup>13</sup>

<sup>d</sup> Slope in Schild plot analysis was set to 1. Results of Schild plot analysis with observed slope  $m$  (cpd.,  $m$ ,  $pA_2$ ): **3**, 0.8, 8.37; **17**, 1.3, 7.50; **19**, 1.3, 7.88; **20**, 1.8, 7.46; **38**, 1.3, 7.56; **45**, 1.7, 7.83.

curves at gpH<sub>1</sub>R are shown (Fig. 1C). For some ligands, for example, **19**, the dose-response curves show a strong depression at higher ligand concentrations. A reason for this partially insurmountable antagonism may be a slow rate of dissociation kinetics of the antagonist, resulting in hemi-equilibrium conditions.<sup>19</sup> In general, the  $pA_2$  values at gpH<sub>1</sub>R are higher, than the  $pK_i$  values at hH<sub>1</sub>R.

For compounds **16–21**, **26**, **38** and **45**, the  $pA_2$  values are found in a range from about 7.7 up to 8.4, whereas the  $pK_i$  values at hH<sub>1</sub>R are found in a range from about 6.1 up to 8.3. There might be two reasons for these differences: First, the data at gpH<sub>1</sub>R are functional data obtained from isolated organ experiments, whereas the data at hH<sub>1</sub>R are binding data. Secondly and more importantly, species differences between hH<sub>1</sub>R and gpH<sub>1</sub>R should be taken into account. Asn<sup>2.61</sup>, for example, was identified to be responsible for species differences between hH<sub>1</sub>R and gpH<sub>1</sub>R, especially in case of long and bulky ligands.<sup>20</sup>

All analyzed hybrid compounds **16–21**, **26**, **38** and **45** exhibit only low affinity to hH<sub>4</sub>R in a range of about 4.5 to 5.2. Thus, compared to JNJ7777120 or to the corresponding JNJ-analogues **5** and **6**, the affinity is significantly decreased (Fig. 3). The introduction of a chlorine into the indole moiety of **5**, leading to JNJ7777120 (compd **2**), results in a significant increase in affinity at hH<sub>4</sub>R.<sup>11</sup> Corresponding structure-activity relationships could not be observed for the analogue series **16–17** and **19–20** (Fig. 3). Two reasons may explain the experimental data: The hH<sub>4</sub>R does not tolerate any linker and/or linked groups. Furthermore, it can be speculated that the binding mode of the JNJ-partial structures in the hybrid compounds at hH<sub>4</sub>R might be different to the JNJ-derivatives itself. In literature, two completely different binding modes for JNJ-derivatives at H<sub>4</sub>R are described. Within a modelling study, an interaction of the indole-NH with Asp<sup>3.32</sup> and an interaction of the positively charged piperazine moiety with Glu<sup>5.46</sup> is suggested.<sup>21</sup> A different binding mode, the positively charged piperazine moiety interacting with Asp<sup>3.32</sup>, was found within an other modelling study.<sup>11</sup> In this case, the indole moiety is embedded in a small pocket between Glu<sup>5.46</sup> and Trp<sup>6.48</sup>.<sup>11</sup> With the latter binding mode, structure-activity relationships of JNJ-derivatives with different substitution patterns in the indole moiety could be explained.<sup>11</sup> In compounds **19** and **38**, the mepyramine partial structure is connected differently to the JNJ partial structure. Compound **19** should show affinity to hH<sub>4</sub>R, if the binding mode of JNJ7777120 presented by Schneider et al is energetically preferred.<sup>11</sup> Here, the piperazine moiety is suggested to interact with Asp<sup>3.32</sup>. Thus, there is space left in the binding pocket in direction to TM II for a ligand elongation at the piperazine moiety. In contrast, compound **38** should show affinity to hH<sub>4</sub>R, if the binding mode of JNJ7777120 presented by Jojart et al. is energetically preferred.<sup>21</sup> Here, the indole moiety is suggested to interact with Asp<sup>3.32</sup>. Thus, there is space left in the binding pocket in direction to TM II for a ligand elongation at the indole moiety. Unfortunately, both compounds, **19** and **38**, exhibit only poor affinity to hH<sub>4</sub>R. One reason for the poor affinity of **38** to hH<sub>4</sub>R, might be a wrong connection point of the mepyramine with the indole moiety. It can be speculated that a different aromatic substitution position might lead to higher affinities at hH<sub>4</sub>R. However, it is noteworthy, that a JNJ derivative with an amino moiety in 5-position ((5-amino-1*H*-indol-2-yl)(4-methylpiperazin-1-yl)methanon) is described in literature<sup>5</sup> with an  $pK_i$  value of about 7.8 at hH<sub>4</sub>R. In contrast, in our competition binding assay, a  $pK_i$  of  $6.80 \pm 0.13$  was determined. In general, the data within this study show that more experimental and modeling studies at hH<sub>4</sub>R have to be performed, in order to get a more detailed insight into interaction of ligands with hH<sub>4</sub>R on molecular level.

In order to obtain information, if the hybrid compounds act as partial agonists, antagonists or inverse agonists at hH<sub>4</sub>R, we performed for two selected compounds **16** and **19** a GTP $\gamma$ S-assay (Fig. 1B, Table 4).

The data revealed, that **16** acts as a partial agonist at hH<sub>4</sub>R, whereas **19** shows inverse agonism (Fig. 1B). The partial agonism of **16** at hH<sub>4</sub>R is unexpected, since mepyramine and JNJ7777120 were identified as inverse agonists at hH<sub>4</sub>R.<sup>7,22</sup>

A comparison of the pharmacological data between hH<sub>1</sub>R and hH<sub>4</sub>R shows, that the H<sub>1</sub>R tolerates the linking of an H<sub>1</sub>R antagonist

**Table 2**  
Calculated interaction energies between ligand and hH<sub>1</sub>R or ligand and internal water for compounds **16**, **19** and **38**

	C LR (kJ/mol)	LJ LR (kJ/mol)	C LW (kJ/mol)	LJ LW (kJ/mol)	C+LJ LR (kJ/mol)	C+LJ LW (kJ/mol)	C+LJ LR+LW (kJ/mol)
<b>16</b>	-157 ± 1	-252 ± 1	-119 ± 1	-32 ± 1	-409 ± 2	-151 ± 2	-560 ± 2
<b>19</b>	-197 ± 1	-253 ± 1	-186 ± 1	-47 ± 1	-450 ± 2	-233 ± 2	-683 ± 2
<b>38 (R)</b>	-166 ± 1	-286 ± 1	-94 ± 1	-51 ± 1	-452 ± 2	-145 ± 2	-597 ± 2
<b>38 (S)</b>	-243 ± 1	-286 ± 1	-43 ± 1	-33 ± 1	-529 ± 2	-76 ± 2	-605 ± 2

The interaction energies were calculated with GROMACS. C: Coulomb (short range); LJ: Lennard–Jones (short range); LR: interaction between ligand and hH<sub>1</sub>R; LW: interaction between ligand and internal water.

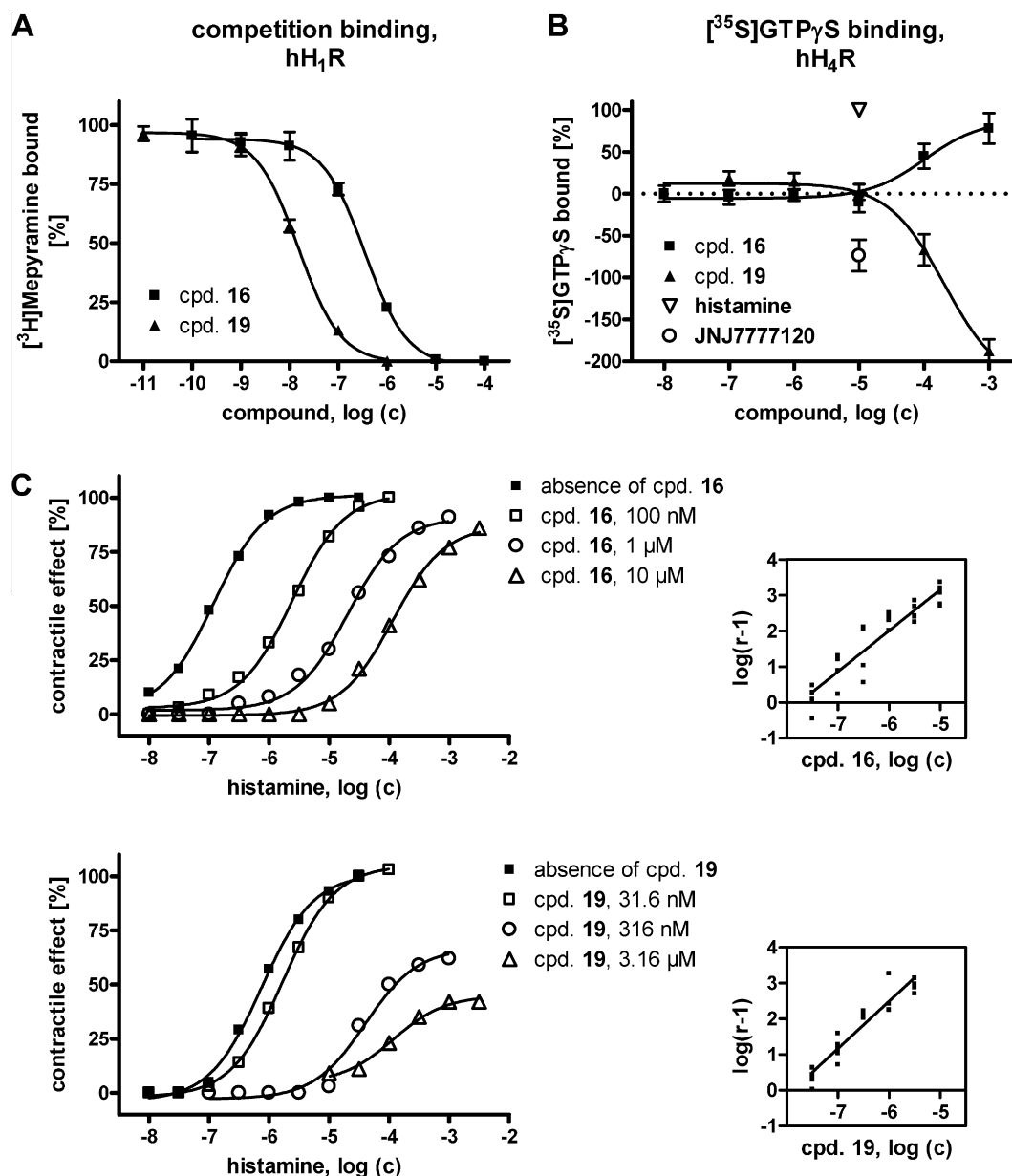


**Figure 1.** (A) Competition binding isotherms for compounds **16** and **19** at hH<sub>1</sub>R, coexpressed with RGS4 in Sf9 cell membranes. (B) Functional GTPγS binding assay for compounds **16** and **19** at hH<sub>4</sub>R-RGS19 coexpressed with Gα<sub>12</sub> and Gβ<sub>1</sub>γ<sub>2</sub> in Sf9 cell membranes. (C) Contraction of guinea-pig ileum (whole segments) by histamine in absence and presence of the inhibitors **16** and **19**. Inset: Schild plot for the corresponding inhibitor.

to JNJ7777120. But affinity is dependent from linker length. In contrast, the hH<sub>4</sub>R does not tolerate linked pharmacophores, since the affinity of all analyzed hybrid compounds was significantly decreased compared to JNJ7777120. All hybrid compounds were antagonists at gpH<sub>1</sub>R. In contrast, the hH<sub>4</sub>R is sensitive with regard to linker length concerning the efficiency. Here, the linker length acts

as a partial (**16**)–inverse (**19**) agonism switch at hH<sub>4</sub>R. Thus, linker length has completely different influences onto pharmacology of hH<sub>1</sub>R and hH<sub>4</sub>R.

Within this study we presented new hybrid compounds with different H<sub>1</sub>- and H<sub>4</sub>-pharmacophores. These compounds showed (high) affinity to hH<sub>1</sub>R, but rather low affinity to hH<sub>4</sub>R. However,

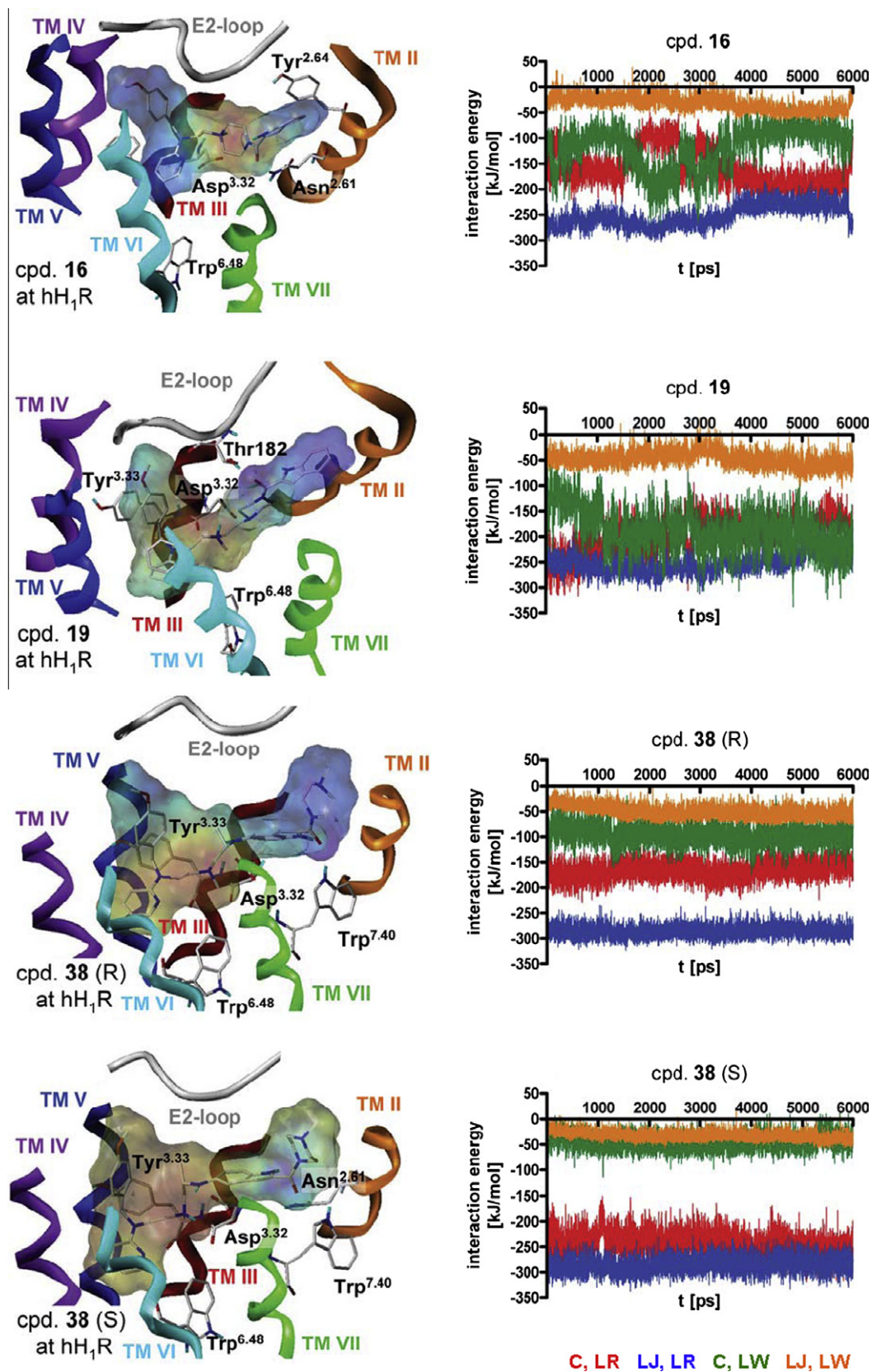


**Figure 2.** Binding mode of **16**, **19** and **38** at hH<sub>1</sub>R and interaction energy between **16**, **19** or **38** with hH<sub>1</sub>R or internal water, obtained by molecular dynamics.

similar studies with regard to H<sub>1</sub>/H<sub>2</sub>-hybrid compounds showed that high affinity to both receptors is only achieved for distinct H<sub>1</sub>/H<sub>2</sub>-pharmacophores.<sup>8,9</sup> Thus, the connection of H<sub>1</sub>-antagonis-

tic pharmacophores with H<sub>4</sub>-pharmacophores, different from the JN] partial structure may lead to compounds with high affinity to both, H<sub>1</sub>R and H<sub>4</sub>R. However, this study revealed

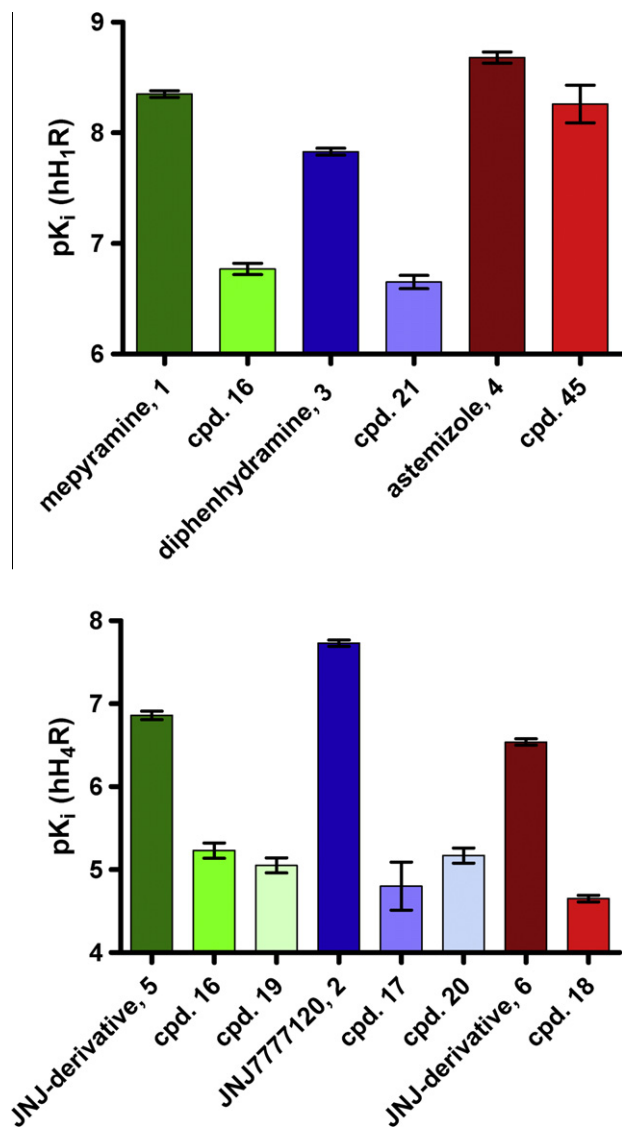


Figure 3. Trends in affinities at hH<sub>1</sub>R and hH<sub>4</sub>R.

Table 3

Calculated Gibbs energy of solvation for compounds **16**, **19** and **38** in water and in the binding pocket of hH<sub>1</sub>R

	$\Delta G_{\text{sol}}^0$ (L, wat)	$\Delta G_{\text{sol}}^0$ (L, hH <sub>1</sub> R)	$\Delta\Delta G_{\text{sol}}^0$ (water→hH <sub>1</sub> R)
<b>16</b>	$-171 \pm 2$	$-446 \pm 21$	$-275 \pm 23$
<b>19</b>	$-145 \pm 3$	$-436 \pm 16$	$-291 \pm 19$
<b>38</b> (R)	$-248 \pm 4$	$-515 \pm 18$	$-267 \pm 22$
<b>38</b> (S)	$-243 \pm 3$	$-507 \pm 16$	$-264 \pm 19$

The calculations were performed, based on the thermodynamic integration method, using the coupling parameter  $\lambda$ , switching on, respectively off the interaction between ligand and surrounding, as described previously.<sup>18</sup>  $\Delta G_{\text{sol}}^0$  (L, wat) corresponds to the Gibbs energy of solvation of the ligand L in water,  $\Delta G_{\text{sol}}^0$  (L, hH<sub>1</sub>R) corresponds to the Gibbs energy of solvation of the ligand L in the binding pocket of hH<sub>1</sub>R and  $\Delta\Delta G_{\text{sol}}^0$  (water→hH<sub>1</sub>R) corresponds to the change in Gibbs energy of solvation for transferring the ligand from water into binding pocket of hH<sub>1</sub>R

important insights into structure–activity relationships at hH<sub>1</sub>R and hH<sub>4</sub>R.

Table 4

Efficacies of selected compounds **16** and **19** in the GTP $\gamma$ S-assay at hH<sub>4</sub>R

	Potency pEC <sub>50</sub>	Efficacy E <sub>max</sub> (%)
histamine	n.d.	1.00 <sup>a</sup>
JNJ7777120, <b>2</b>	n.d.	$-0.74 \pm 0.19$ <sup>b</sup>
<b>16</b>	$3.98 \pm 0.31$	$0.88 \pm 0.18$
<b>19</b>	<4 <sup>c</sup>	<-1 <sup>c</sup>

<sup>a</sup> The efficacy of histamine was determined at a concentration of 10  $\mu$ M and set to 1.00 (pEC<sub>50</sub> =  $7.86 \pm 0.20$ <sup>22</sup>)

<sup>b</sup> The efficacy of JNJ7777120 was determined at a concentration of 10  $\mu$ M and was determined relative to the efficacy of histamine (pEC<sub>50</sub> =  $7.80 \pm 0.21$ , E<sub>max</sub> =  $-0.59$ <sup>22</sup>)

<sup>c</sup> A rapid decrease in [<sup>35</sup>S]GTP $\gamma$ S binding was observed for concentrations of **19** greater than 100  $\mu$ M, thus, neither potency nor efficacy could be determined exactly.

## Acknowledgments

We are grateful to Christine Braun, Kerstin Röhl and Gertraud Wilberg for expert technical assistance. This work was supported by the Deutsche Forschungsgemeinschaft (Project STR 1125/1-1 and the Graduate Training Program (Graduiertenkolleg) GRK 760, ‘Medicinal Chemistry: Molecular Recognition–Ligand–Receptor Interactions’).

## Supplementary data

Supplementary data associated with this article can be found, in the online version, at doi:10.1016/j.bmcl.2011.09.001.

## References and notes

- Thurmond, R. L.; Gelfand, E. W.; Dunford, P. J. *Nat. Rev. Drug Disc.* **2008**, *7*, 41.
- Dunford, P. J.; O'Donnell, N.; Riley, J. P.; Williams, K. N.; Karlsson, L.; Thurmond, R. L. *J. Immunol.* **2006**, *176*, 7062.
- Rosbach, K.; Stark, H.; Sander, K.; Leurs, R.; Kietzmann, M.; Bäumer, W. *Vet. Dermatol.* **2009**, *20*, 555.
- Parsons, M. E.; Ganellin, C. R. *Br. J. Pharmacol.* **2006**, *147*, S127.
- Jablonowski, J. A.; Grice, C. A.; Chai, W.; Dvorak, C. A.; Venable, J. D.; Kwok, A. K.; Ly, K. S.; Wei, J.; Baker, S. M.; Desai, P. J.; Jiang, W.; Wilson, S. J.; Thurmond, R. L.; Karlsson, L.; Edwards, J. P.; Lovenberg, T. W.; Carruthers, N. I. *J. Med. Chem.* **2003**, *46*, 3957.
- Schnell, D.; Brunskole, I.; Ladova, K.; Schneider, E. H.; Igel, P.; Dove, S.; Buschauer, A.; Seifert, R. *Naunyn-Schmied Arch. Pharmacol.* **2011**, *383*, 457.
- Deml, K. F.; Beermann, S.; Neumann, D.; Strasser, A.; Seifert, R. *Mol. Pharmacol.* **2009**, *76*, 1019.
- Schulze, F. R.; Buschauer, A.; Schunack, W. *Eur. J. Pharm. Sci.* **1998**, *6*, 177.
- Wolf, C.; Schulze, F. R.; Buschauer, A.; Schunack, W. *Eur. J. Pharm. Sci.* **1998**, *6*, 187.
- Strasser, A.; Striegl, B.; Wittmann, H.-J.; Seifert, R. *J. Pharmacol. Exp. Ther.* **2008**, *324*, 60.
- Schneider, E. H.; Strasser, A.; Thurmond, R. L.; Seifert, R. *J. Pharmacol. Exp. Ther.* **2010**, *334*, 513.
- Schneider, E. H.; Schnell, D.; Papa, D.; Seifert, R. *Biochemistry* **2009**, *48*, 1424.
- Elz, S.; Kramer, K.; Pertz, H. H.; Detert, H.; ter Laak, A. M.; Kühne, R.; Schunack, W. *J. Med. Chem.* **2000**, *43*, 1071.
- Cherezov, V.; Rosenbaum, D. M.; Hanson, M. A.; Rasmussen, S. G.; Thian, F. S.; Kobilka, T. S.; Choi, H. J.; Kuhn, P.; Weis, W. I.; Kobilka, B. K.; Stevens, R. C. *Science* **2007**, *318*, 1258.
- Strasser, A.; Wittmann, H.-J. *J. Comput. Aided Mol. Des.* **2010**, *24*, 759.
- Shimamura, T.; Han, G. W.; Shiroishi, M.; Weyand, S.; Tsujimoto, H.; Winter, G.; Katritch, V.; Abagyan, R.; Cherezov, V.; Liu, W.; Kobayashi, T.; Stevens, R.; Iwata, S. *Nature* **2011**, *475*, 65.
- Wittmann, H.-J.; Seifert, R.; Strasser, A. *Mol. Pharmacol.* **2009**, *76*, 25.
- Wittmann, H.-J.; Strasser, A.; Seifert, R. *Naunyn Schmied Arch. Pharmacol.* **2011**, *384*, 287.
- Kenakin, T.; Jenkinson, S.; Watson, C. J. *Pharmacol. Exp. Ther.* **2006**, *319*, 710.
- Bruysters, M.; Jongejan, A.; Gillard, M.; van de Manakker, F.; Bakker, R. A.; Chatelain, P.; Leurs, R. *Mol. Pharmacol.* **2005**, *67*, 1045.
- Jojart, B.; Kiss, R.; Viskolcz, B.; Keseru, G. M. *J. Chem. Inf. Model* **2008**, *48*, 1199.
- Sander, K.; Kottke, T.; Tanrikulu, Y.; Proschak, E.; Weizel, L.; Schneider, E. H.; Seifert, R.; Schneider, G.; Stark, H. *Bioorg. Med. Chem.* **2009**, *17*, 7186.